



---

---

**FORMATION OF COPPER OXIDE NANOPARTICLES USING GREEN  
SYNTHESIS THROUGH NEEM LEAF (*AZADIRACHTA INDICA*)  
EXTRACT**

**G. PUNITHAKUMARI<sup>1\*</sup>, V. PREETHI<sup>2</sup>, D. ISHWARYA<sup>2</sup>, E. MOHANA<sup>2</sup> AND S.  
MEENA<sup>2</sup>**

**1:** Department of Chemistry, K.Ramakrishnan College of Engineering (A), Tiruchirappalli-  
621112, Tamilnadu, India

**2:** Department of Chemistry, Theivanai Ammal College for Women (A) Villupuram-  
605602. Tamilnadu, India

**\*Corresponding Author: Dr. G. Punithakumari: E Mail: [gpunithababu@gmail.com](mailto:gpunithababu@gmail.com)**

Received 15<sup>th</sup> Feb. 2023; Revised 25<sup>th</sup> April 2023; Accepted 14<sup>th</sup> July 2023; Available online 1<sup>st</sup> March 2024

<https://doi.org/10.31032/IJBPAS/2024/13.3.7857>

**ABSTRACT**

Nowadays green technology plays the major role for generating the nanoparticles towards the researchers with low cost method. Copper sulphate 0.1M and neem extract was made as a bulk solution. 150ml of neem extract and 50ml of copper sulphate is taken and mixed it well and thus the solution is taken in the beaker. Green Synthesis and Characterisation of Copper Oxide Nanoparticles using *Azadirachta indica* (Neem) Leaf Aqueous Extract can reduce copper ions into copper nano particles within 5 minutes of reaction time and brown coloured precipitate settling down. The biosynthesized nanoparticles of copper oxide are characterized through UV-Vis spectra, FT-IR, and XRD. In UV-Vis spectra a peak was obtained at 346 nm due to inter band transition of core electrons and band gap energy of 2.65 eV was observed through tauc plot. Sharp peak at 480.42 and 538.80 cm<sup>-1</sup> in FT-IR spectrum is due to Cu-O bond. CuO Nano particle is crystalline and identical to simple cubic. The particle sizes of CuO NPs are found in different sizes range of 49 nm, 87 nm, 120 nm and 324 nm.

**Keywords: Copper Oxide Nanoparticles, Green Synthesis, Neem Leaf (*Azadirachta indica*)**

## 1. INTRODUCTION

Nanoscience is the branch of science that deals with the study of materials at the scale of nanometer (1-100 nm) at least in one dimension [1-3]. Nanotechnology on the other hand, concerns itself with tools and techniques of manipulating the nanoscale objects at molecular level [4]. Nanoscale objects or nanomaterials attain immense importance because of their superior chemical, physical, optical, magnetic, thermal, electrical, imaging and unique properties they are highly in various disciplines like agriculture, catalysis mechanical properties compared to their conventional counterparts [5-7]. Because of these, chemistry, electronics, environmental sectors, food industry, physics, solar cells and also in biomedical healthcare [8]. Acquiring the knowledge from nanoscience about the material behavior of nanoscale objects, nanotechnology focuses on engineering various nanomaterials for widespread applications [9] in the field of photonics, electronics and medicines [8]. Specially in the field of medicine, numerous nanoplatforms have been explored extensively for biosensing, bioimaging drug delivery, gene therapy, tissue engineering and nanomedicine [10]. Copper nanoparticles have drawn much attention because of their natural abundance, good electrical conductivity, high melting point, minimal electrochemical migration,

excellent soldering ability, catalytic activity and affordability [11]. Copper has substituted the place of other metals such as Ag, Au and Pt, in many applications like, heat transfer and inkjet printing [12], because of its low cost, high conductivity [13], small size, high surface/volume ratio, improvement of size, shape and oxidation resistance, etc. [14]. Moreover, high boiling point of copper helps to withstand high-temperature and- pressure chemical reactions and thus helps in various organic transformations [15]. All these distinctive properties, have made copper one of the most precious metals in recent years.

In literature, the Cu nanoparticles are synthesized from vapour deposition [16], electrochemical reduction [17], radiolysis reduction [18], thermal decomposition [19], chemical reduction of copper metal salt [20], and room temperature synthesis using hydrazine hydrate and starch [21]. In recent, green synthesis of Cu nanoparticles was achieved by using plant extract [22]. Neem leaves play a vital role in arresting disease pathogens and neem has an anti-inflammatory properties, treat fungal infection, useful in detoxification and it also prevents gastrointestinal disease, treat wounds and strengthening immune system [23-28]. Neem leaves play a vital role in arresting disease pathogens and neem has an anti-inflammatory properties, treat fungal infection

[29-33], useful in detoxification and it also prevents gastrointestinal disease, treat wounds and strengthening immune system.

## 2. Experimental Methods

### 2.1. Collection of Sample

*Azadirachta indica* (neem) leaves were collected within the College campus, villupuram. Then we separate the leaves and taken the healthy leaves for the rest which is shown in **Figure 1**.



Figure 1: *Azadirachta indica* (neem) leaves

### 2.2. Preparation of Extract

The selected leaves were washed in running tap water and then again washed with distilled water. Then the leaves were dried with absorbent paper. These leaves were dried for 2 days. About 25 g of neem leaves was weighed and taken in a beaker and 250 ml of distilled water was added to it. This was heated for 1 hour at 60 °C. By this time aqueous part turns yellow. The extract was filtered by Whatmann No.1 filter paper. This filtrate was made upto 250 mL in a standard measuring flask. It was then stored in refrigerator for further use.

### 2.3. Chemicals and Instruments for the study of nanoparticles

Copper sulphate ( $\text{CuSO}_4 \cdot 5\text{H}_2\text{O}$ ) was obtained from Nice Chemicals. Freshly

prepared distilled water was used throughout the experiment. UV-Vis spectrometer (Jasco V-530) and FT-IR (Thermo Scientific Nicolet iS5) were used for characterisation. Surface analysis done by Nanosurf Easy scan 2 AFM. The structure were analyzed by scanning electron microscopy (SEM, Hitachi S-2500C) and high resolution transmission electron microscopy (HR-TEM; JEOL-2010). Copper concentrations were determined using inductively coupled plasma spectrometry (ICP, JY38Plus).

### 2.4. Synthesis of CuO Nanoparticles

For the synthesis of Copper oxide nanoparticles 50 mL of copper sulphate and 150 mL of Neem extract is taken and mixed in a beaker. When mixed it is observed that

the colour is dark green and brown coloured precipitate is settling down. This obtained precipitate is filtered using Whatmann no- 1

filter paper, washed with distilled water and left overnight to dry. The next day CuO nanoparticles were collected (**Figure 2**).

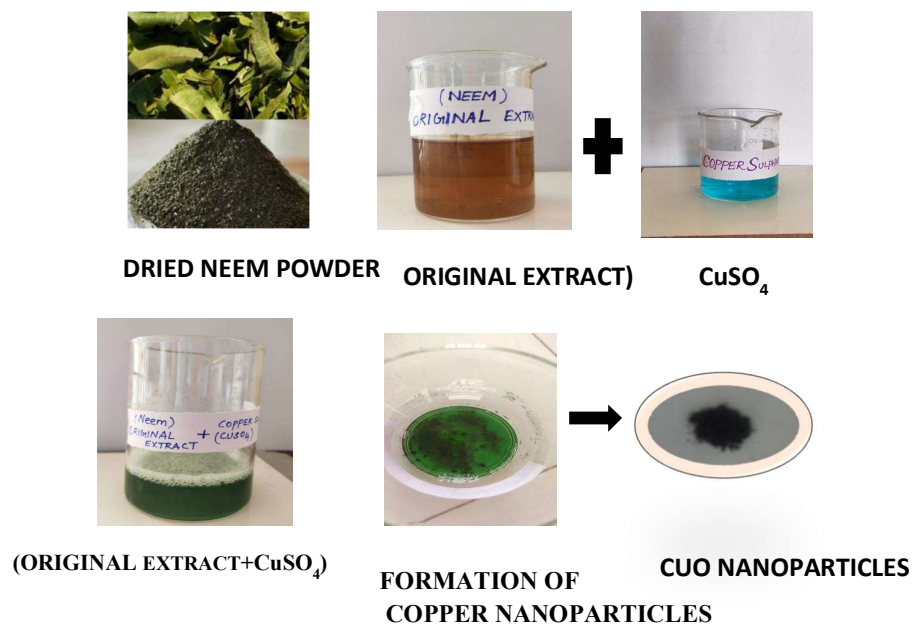


Figure 2: CuO Nanoparticles synthesis method

## RESULTS AND DISCUSSION

Reduction of the copper ion to copper nanoparticles during exposure to the plant leaf extract could be followed by color change and thus UV-vis spectroscopy. It is observed that the maximum absorbance occurs at 560 nm and steadily increases in intensity as a function of reaction time. We quantitatively monitored the concentrations of copper nanoparticles and conversion by measuring the absorbance at 560 nm. The linear relationship was obtained between the copper concentration determined by ICP and the absorbance at 560 nm. TEM images obtained with 15 - 20% Neem leaf broth and 1 mM  $\text{CuSO}_4 \cdot 5\text{H}_2\text{O}$  solution showed that relatively spherical nanoparticles are formed

with diameter of 45 - 110 nm. As the reaction temperature increased, both synthesis rate and conversion to copper nanoparticles increased [34-35]. The conversion after 24 hr was about 70% at 25°C and 80 - 100% at 60 and 95 °C. The average particle size decreased from 110 nm at 25°C to 45 nm at 95°C. Regarding the reason of decrease in particle size with temperature, we can hypothesize as follows. As the reaction temperature increases, the reaction rate increases and thus most copper ions are consumed in the formation of nuclei, stopping the secondary reduction process on the surface of the preformed nuclei. Similar trends were observed with gold and silver nanoparticles synthesized

using plant extracts. Effects of different neem leaf broth concentrations at 5 - 20% were investigated on copper nanoparticles formation at 1 mM  $\text{CuSO}_4 \cdot 5\text{H}_2\text{O}$ . The reaction rate was highest at 20% leaf broth concentration. With increasing the leaf broth concentration, the average particle size decreased up to 15% leaf broth concentration and then increased at 20% leaf broth concentration. Effects of  $\text{CuSO}_4 \cdot 5\text{H}_2\text{O}$  concentration were also investigated on conversion to copper nanoparticles obtained with 15% neem broth concentration. The times required for more than 90% conversion were 1600, 1400, and 300 min at 95 °C, respectively, when  $\text{CuSO}_4 \cdot 5\text{H}_2\text{O}$  concentrations were 0.5, 1, and 2 mM, respectively. The average particle size decreased with increasing the  $\text{CuSO}_4 \cdot 5\text{H}_2\text{O}$  concentration. It is considered that particle size is dependent on various conditions such as reaction temperature, leaf broth concentration and  $\text{CuSO}_4 \cdot 5\text{H}_2\text{O}$  concentration. EDS profile showed copper signals along with oxygen and carbon peak, which may originate from the biomolecules that are bound to the surface of the copper nanoparticles. EDX spectrum showed characteristic copper peaks, suggesting that copper nanoparticles were successfully synthesized using neem leaves.

### 3.1 FT-IR discussions of copper nanoparticle

FT-IR graph is taken in the range of 400 to 1500. In **Figure 3**, FT-IR spectra peaks at 480.42, 538.80, 811.73, 887.54, 1072.5, 1210.85, 1273.69, 1488.86  $\text{cm}^{-1}$ . There is sharp peak observed at 480.42 and 538.80  $\text{cm}^{-1}$  in the spectrum of CuO nanoparticles which is the characteristics of Cu-O bond formation. Other peak due to impurity from neem extract.

### 3.2 Synthesis of CuO nanoparticles and UV-Visible analysis

In the current work, *Neem* leaves extract was used for the synthesis of stable Cu nanoparticles in aqueous phase. The formations of CuNPs were confirmed using UV-visible spectra due to surface plasmon resonance. The UV-visible absorption spectra of synthesized CuNPs were recorded at fixed wavelengths from 200 to 800 nm. The UV spectrum of neem leaves extract shows absorption bands at 338 and 226 nm, which is characterized due to the absorbance of benzoyl-related systems of the biomolecules. The characteristic absorption peak of Cu colloids was observed at 588 nm, as shown in **Figure 4**. Surface plasmon is the electron excitation in the conduction band of the nanoparticles surface. The metal nanoparticles providing the characteristic absorption spectra in the UV-visible region are called surface plasmon resonance of nanoparticles. It has been reported in the literature that the surface plasmon resonance band of Cu nanoparticles provides

absorption from 570 to 600 nm. The CuNPs surface plasmon band stability at 588 nm confirms the formation of Cu nanoparticles and shows that particles in the solution are monodispersed with no sign of agglomeration.

### 3.3 FE-SEM analysis of CuO nanoparticles

For identification of size and surface morphology, FE-SEM was used. FE-SEM images of the green synthesized CuNPs were found to be spherical in shape without aggregation (**Figure 5**). From the images, it has been confirmed that the synthesized CuNPs are stabilized by biomolecules present in *neem leaves* extract. It has been reported in the literature 21 that the optical and electronic properties of metal nanoparticles are shape dependant. For size and surface morphology determination, FE-SEM has previously been used by several investigators for the characterization of metal nanoparticles. The average size of the synthesized CuNPs was found to be 70 nm having monodispersity. Higher magnification FE-SEM images show the well-defined surface modification and

coating of biomolecules, which stabilize the fine surface of CuNPs.

### 3.4. XRD ANALYSIS OF CuNPs

The XRD patterns of *neem leaves* synthesized CuNPs is shown in **Figure 6**, The XRD pattern of the synthesized CuNPs is similar to previous reports. All the possible peaks observed indicate metallic copper, which also show the polycrystalline nature of CuNPs. In the XRD pattern, two distinct diffraction peaks for CuNPs are observed with a  $2\theta$  value of  $43.74^\circ$  and  $50.78^\circ$  representing Bragg's reflections of an planes of fcc crystal structures of CuNPs. The average crystallites size of copper was calculated from the Scherrer equation. The average crystallite size of the CuNPs was 76 nm, which is ably supported by high-resolution FE-SEM images as well. The small diffraction peak at  $35.5^\circ$ , which corresponds to the Bragg's reflections of [002] may be due to the formation 22 of copper oxide. Here, the formation of copper oxide in small quantities cannot be ignored. Some unidentified peaks at  $29.05^\circ$ ,  $38.2^\circ$ ,  $41.53^\circ$ , and  $42.53^\circ$  were assigned (\*). These unassigned peaks might be due to the crystallization of biomolecules.

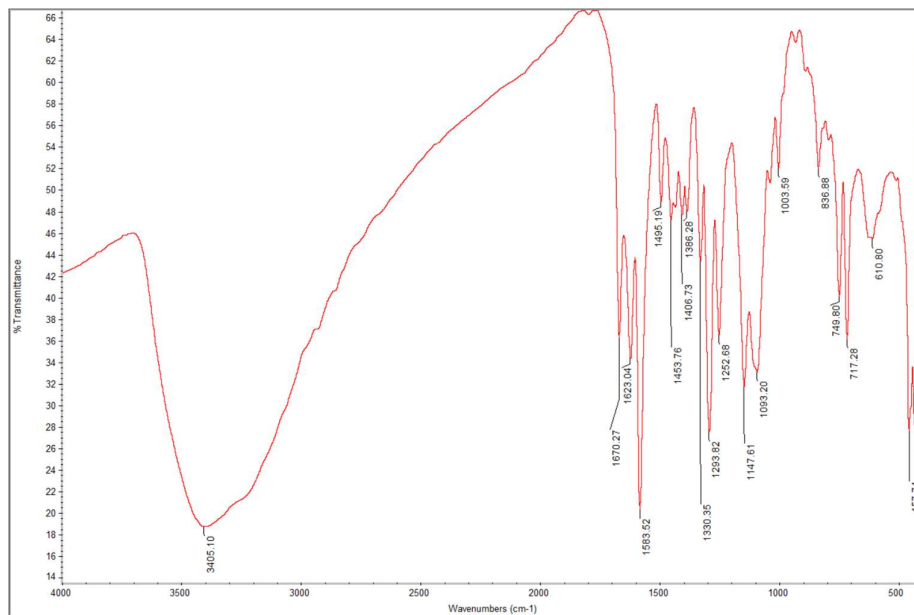


Figure 3: FT-IR Spectra of CuO Nano particles

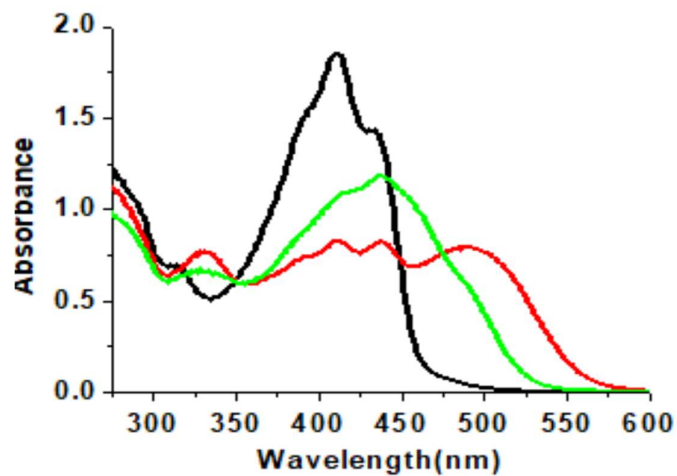


Figure 4: UV-visible spectra of neem leaves extract and synthesized CuNP

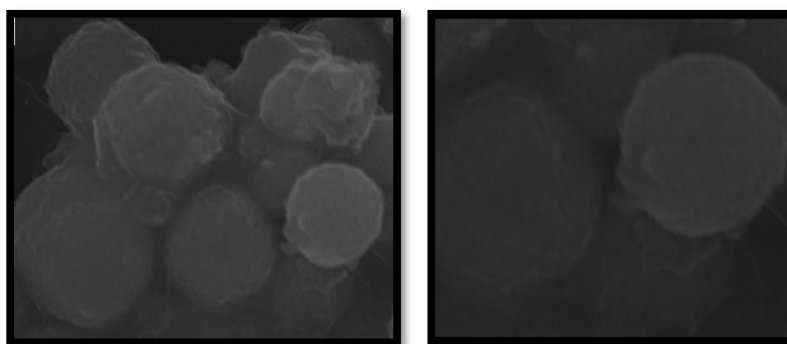
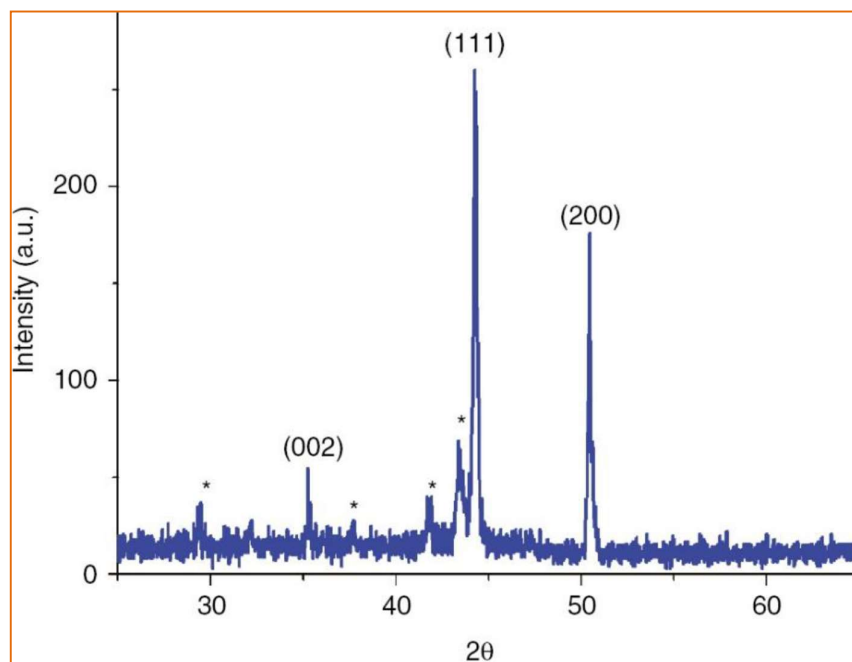


Figure 5: FE-SEM images of prepared CuNPs



#### 4. CONCLUSION

In conclusion, these methods are easily available starting materials, inexpensive and procedure is easy to carry out any laboratory, use of toxic reagent is avoided and pollution free, here we report eco-friendly synthesis of CuO NPs using a leaf extract of *Azadirachta indica* (Neem). Here, CuNPs were successfully prepared for the first time using *neem leaves* extract, in which the plant extract acts as a capping as well as a reducing agent. Initially, the formation of nanoparticles was confirmed through UV-visible spectrophotometer. FT-IR spectra confirmed that biomolecules of *neem leaves* were responsible for the reduction capping of CuNPs. The prepared CuNPs were structurally and morphologically characterized by using FE-

SEM, EDX, and XRD. Considering the excellent catalytic performance; the prepared CuNPs catalyst can be synthesized in large quantities due to their low cost, high stability and reusability, and environmentally friendly plant support and thus can be used for the purification of natural water from organic effluents.

#### 5. REFERENCES

- [1] Qu, X.; Li, Y.; Li, L.; Wang, Y.; Liang, J.; Liang, J. *Journal of Nanomaterials*, 2015.
- [2] Dreaden, E. C.; Alkilany, A. M.; Huang, X. C.; Murphy, J.; El-Sayed, M. A. *Chemical Society Reviews*, 2012, 41 (7), 2740–2779.
- [3] Zhang, L.; Webster, T. J. *Nano Today*, 2009, 4, 66-80.
- [4] Roco, M. C. *Current Opinion in*

- Biotechnology, 2003, 14:337–346.
- [5] Sapsford, K. E.; Algar, W. R.; Berti, L.; Gemmill, K. B.; Casey, B. J.; Oh, E.; Stewart, M. H.; Medintz, I. L. *Chem. Rev.* 2013, 113 (3), 1904–2074.
- [6] Ealias, A. M. and Saravanakumar M P. *Materials Science and Engineering*, 2017, 263, 032019.
- [7] Yan, Q-L.; Gozin, M.; Zhao, F-Q.; Cohen, A. and Pang, S-P. *Nanoscale*, 2016, 8, 4799–4851.
- [8] Li, Y.; Wang, Y.; Huang, G. and Gao, J. *Chem. Rev.* 2018, 118, 5359–5391.
- [9] Jiang, S.; Win, K. Y.; Liu, S.; Teng, C. P.; Zheng, Y.; Han, M.-Y. *Nanoscale*. 2013, 5 (8), 3127.
- [10] Tao, Y.; Li, M.; Ren, J.; Qu, X. *Chem. Soc. Rev.* 2015, 44, 8636–8663.
- [11] Machado S, Pacheco J G, Nouws H P A, Albergaria J T and Delerue-Matos C. *Sci. Total Environ.* 2015, 533, 76–81.
- [12] James K. Carrow, Akhilesh K. Gaharwar. *Macromol. Chem. Phys.* 2015, 216, 248–264
- [13] Ayuk, E. L.; Ugwu M. O.; Samuel A.B. *Chemistry Research Journal*, 2017, 2(5): 97-123.
- [14] Tiwari, D K.; Behari, J. and Sen, P. *World Applied Sciences Journal*, 2008, 3(3): 417-433.
- [15] Falagan-Lotsch, P.; Grzincic, E. M.; & Murphy, C. J. *Bioconjugate Chemistry*, 2017, 28(1), 135–152.
- [16] Bhaviripudi, S.; Mile, E.; Iii, S A S.; Zare, A T.; Dresselhaus, M S.; Belcher, A M.; and Kong, J. *Catalysts*. 2007, 1516–7.
- [17] Gawande, M. B.; Goswami, A.; Felpin, F.-X.; Asefa, T.; Huang, X.; Sila Varma, R. S. *Chemical Reviews*, 2016, 116 (6), 3722–3811.
- [18] Salavati-niasari, M.; Davar, F.; and Mir, N. *Polyhedron*, 2008, 27, 3514–8.
- [19] Tamilvanan, A.; Balamurugan, K.; Po nappa, K.; & Kumar, B. M. *International Journal of Nanoscience*, 2014, 13 (02), 1430001.
- [20] Manimaran, R.; Palaniradja, K.; Alagumurthi, N.; Sendhilnathan, S. and Hussain, J. *Appl. Nanosci.* 2013, 4, 163.
- [21] Wang, C.; Wang, C.; Xu, L.; Cheng, H.; Lin, Q.; Jhang, C. *Nanoscale* 2014, 6, 1775–1781.
- [22] Jiang, J.; Kim, S.-H.; Piao, L. *Nanoscale*, 2015, 7, 8299–8303.
- [23] Shelke, S. N.; Bankar, S. R.; Mhaske, G. R.; Kadam, S. S.; Murade, D. K.; *et al.* *ACS Sustainable Chem. Eng.* 2014, 2,

- 1699–1706.
- [24] Scotti, N.; Dangat, M.; Gervasini, A.; Evangelisti, C.; Ravasio, N.; Zaccheria, F. *ACS Catal.* 2014, 4, 2818–2826.
- [25] Shim, I. W.; Noh, W. T.; Kwon, J.; Cho, J. Y.; Kim, K. S.; Kang, D. H. *Bull. Korean Chem. Soc.* 2002, 23, 563–566.
- [26] Vallabani, N. V. S.; & Singh, S. 3 *Biotech*, 2018, 8(6), 279.
- [27] Gupta, AK.; Gupta, M. *Biomaterials*, 2005, 26(18), 3995–4021.
- [28] Gupta, AK.; Naregalkar, RR.; Vaidya, VD.; Gupta, M. *Nanomedicine (Lond)* 2007, 2(1), 23 – 39.
- [29] Ansari, S. A. M. K.; Ficiarà, E.; Ruffinatti, F. Al.; Stura, I.; Argenziano, M.; *et al.* *Materials*, 2019, 12, 465.
- [30] Kharisov, B. I.; Dias, H. V. R.; Kharissova, O.V.; Vazquez, Y. P.; Gomez, I. *RSC Adv.* 2014, 4, 45354–45381.
- [31] Ali, A.; Zafar, H.; Zia, M.; Ul Haq, I.; Phull, A.R.; Ali, J.S.; Hussain, A. *Nanotechnol. Sci. Appl.* 2016, 9, 49–67.
- [32] Laurent, S.; Forge, D.; Port, M.; *et al.* *Chem Rev.* 2008, 108, 2064–2110.
- [33] Cuenya, BR. *Thin Solid Films*, 2010, 518(12), 3127–3150.
- [34] Narayanan, KB.; Sakthivel, N. *Adv Colloid Interface Sci.* 2010, 156(1–2), 1–13.
- [35] Xuan, Y. and Li, Q. *Int. J. Heat and Fluid Flow*, 2000, 21.